PRAMANA
— journal of
physics

Vol. 42, No. 4,
April 1994
pp. 349–363

Analysis of the excitation functions of (α, *xnyp*) reactions on natural copper

N L SINGH, B J PATEL, D R S SOMAYAJULU and S N CHINTALAPUDI*
Physics Department, Faculty of Science, M. S. University, Baroda 390002, India
*IUC-DAEF, Calcutta Centre, 3/LB-8, Bidhan Nagar, Calcutta 700091, India

MS received 17 August 1993; revised 3 January 1994

Abstract. Excitation functions of the reactions ^{63}Cu[(α, n), $(\alpha, 2n) + (\alpha, pn)$] and ^{65}Cu[$(\alpha, n)$, $(\alpha, 2n)$, $(\alpha, 3n)$, $(\alpha, 4n) + (\alpha, p3n)$] were investigated up to 50 MeV using stacked foil activation technique and Ge(Li) gamma ray spectroscopy method. Since natural copper used as the target has two odd-mass stable isotopes of abundance, ^{63}Cu(69·17%) and ^{65}Cu(30·83%), their activation in some cases, gives the same residual nucleus through different reaction channels but with very different threshold energies. In such cases, the individual reaction cross sections are separated with the ratio of theoretical cross sections. The experimental results were compared with the predictions of preequilibrium hybrid model of Blann. A general agreement was found in all reactions using initial exciton number $n_0 = 4(4p0h)$ and also preequilibrium fraction depends on the incident particle energy.

Keywords. Nuclear reactions; ^{63,65}Cu(α, *xnyp*); stacked foil activation technique; $E \leqslant 50$ MeV preequilibrium emission.

PACS No. 25·60

1. Introduction

The preequilibrium reaction mechanism is being used since the last two decades to explain high energy continuum of the ejectile spectrum. The mechanism takes into account the emission of particles during the relaxation process of the target plus projectile composite nucleus towards the statistically equilibrated compound nucleus. The relaxation is assumed to take place through a cascade of two body interactions and ejectile emitted at any stage of the binary cascade constitute the preequilibrium spectra. The preequilibrium process has been extensively studied since the exciton model was proposed by Griffin [1]. The exciton model has been extended and refined through analysis of many experimental data, and several models have been developed within the framework of semiclassical or phenomenological approaches [2–10]. On the other hand fully quantum mechanical theories of preequilibrium processes have been developed by several groups [11–16], which so far been confined to nucleon interactions with not more than two emergent particles. Due to the complexity of computation, for the interaction of complex-particle like an α-particle the quantum mechanical picture is yet to come.

Indeed rather extensive experimental data are available in literature [17–27] for α-induced reactions on copper, mostly using poor resolution detectors i.e. GM counter, scintillation detector and proportional counters. Because of the poor resolution of the detectors there were many inconsistencies in the data. Recently Graf *et al* [24],

Rizvi *et al* [25] Bhardwaj *et al* [26] and Mohan Rao *et al* [27] have also studied α-induced reactions on copper using Ge(Li) detector. In view of the large uncertainties and mutual discrepancies, a reinvestigation of the above reactions was undertaken with the two-fold aim of (i) improving the quality of experimental data and (ii) to test the preequilibrium models with systematic data obtained in the present work.

2. Experimental procedure

The excitation functions of the α-induced nuclear reactions on natural copper were determined by the stacked-foil technique and Ge(Li) gamma ray spectroscopy method. The excitation functions were measured in three steps namely 50–20 MeV, 40–10 MeV and 30–10 MeV, using copper foils of thicknesses 23 mg/cm^2, 8·9 mg/cm^2 and 12 mg/cm^2 respectively together with several aluminium degraders of varying thicknesses to reduce the beam energy to desired levels. These three independent measurements have large overlapping energy regions which enabled us to check the consistency of the measurements. The beam spot on the foil stack was always restricted to 5 mm by a central hole in a 6 mm thick tantalum collimator placed in front of each stack. No catcher foil is used since recoil distribution is small at this energy and falls within experimental errors. The α-beam is totally stopped in the electrically insulated foil stack which is itself serving as a Faraday cup. The total α-particle flux was measured using current integrator. Beam current of the order of 250 nA was maintained for about 1 h in each irradiation. After accounting for the energy degradation in Al-foils, the energy of the alpha beam at half the thickness of the

Table 1. Nuclear data used for identification of residual nuclei [29].

Reaction	Q-value (MeV)	Half-life ($T_{1/2}$)	Gamma ray energy E_γ(keV)	% Abundance (θ_γ)
$^{63}_{29}Cu(\alpha, n)^{66}_{31}Ga$	−7·5	9·45 h	834 1039	6·06 38 ± 2
$^{63}_{29}Cu(\alpha, 2n)^{65}_{31}Ga$	−16·64	15·2 m	153 752	5·98 5·49
$^{63}_{29}Cu(\alpha, pn)^{65}_{30}Zn$	−12·59	244 d ± 0·2	1115·5	50·75 ± 0·10
$^{65}_{29}Cu(\alpha, n)^{68}_{31}Ga$	−5·85	68 m	1077 1261	3·0 ± 0·3 0·09
$^{65}_{29}Cu(\alpha, 2n)^{67}_{31}Ga$	−14·1	78·26 h + 0·07	184·5 300·2	23·56 19·00 ± 1·39
$^{65}_{29}Cu(\alpha, 3n)^{66}_{31}Ga$	−25·3	9·45 h	835 1039	6·06 38 ± 2
$^{65}Cu(\alpha, 4n)^{65}Ga$	−34·37	15·2 m	153 752	5·98 5·49
$^{65}_{29}Cu(\alpha, p3n)^{65}_{30}Zn$	−30·42	244 d ± 0·2	1115·5	50·75 ± 0·10

Error is shown only for those characteristic γ-rays which is used for the evaluation of cross-section.

experimental foil was calculated from range-energy tables of Williamson *et al* [28]. After the irradiation the induced gamma activities in each foil were observed with a high resolution 95 cc Ge(Li) detector (FWHM 2 keV at 1332 keV) coupled with a pre-calibrated 4 k channel Canberra 88 analyser. The residual nuclei were identified using their characteristic γ-rays as mentioned in table 1 [29]. Several spectra were taken at suitable intervals to enable the identification of the half-lives of residual nuclei. The efficiency calibrations of the detector were performed with a calibrated ^{152}Eu source obtained from the Radio-Chemistry division at VECC. The extended source geometry correction has been applied.

2.1 *Cross-section determination*

The formula used in the cross-section calculation was reported in our earlier papers [30, 31].

$$\sigma = \frac{A_r A_{gm} \lambda}{\Phi \theta_r P_r w_i P_i N_{av} (1 - e^{-\lambda t_i}) e^{-\lambda t_w} (1 - e^{-\lambda t_c})} \tag{1}$$

where σ is the cross section for the reaction (mb), A_r is the photopeak area of the characteristic gamma ray of the residual nucleus, A_{gm} is the gram atomic weight of the target element, λ is the disintegration constant of the residual nucleus (s^{-1}), Φ is the flux of the incident particle (No. of particle/cm^2 s), w_i is the weight per unit area of the target foil (g/cm^2), P_i is the fractional abundance by weight of the target isotope of interest, θ_r is the fractional abundance of characteristic gamma ray emitted per decay of the residual nucleus, P_r is the photopeak efficiency of the gamma ray, N_{av} is the Avogadro's number, t_i, t_w and t_c are the periods (s) of irradiation, waiting and counting respectively.

The measured cross-sections for the reactions ^{63}Cu(α, n), ^{63}Cu$(\alpha, 2n)$ + ^{63}Cu(α, pn), ^{65}Cu(α, n), ^{65}Cu$(\alpha, 2n)$ and ^{63}Cu$[(\alpha, 2n) + (\alpha, pn)]$ + ^{65}Cu$[(\alpha, 4n) + (\alpha, p3n)]$ have been listed in table 2. The total error in the experimental cross-section is contributed by photopeak area (1–5%), photopeak efficiency (4–5%), uniformity of the foil thickness (1–2%) spectroscopic data (0·08–8%), the beam current (2–3%). The overall projected error of our measurement is thus between 8–13% for various reactions. The excitation functions for the above reactions are shown in figures 1–4. The horizontal bars show the estimated total energy loss in the actual thickness of the foils, while the vertical flags shown on the cross-sections show the overall error in the measurement.

3. Results and discussion

Consequent on the use of natural copper target which has two odd-mass isotopes of abundances ^{63}Cu(69·17%) and ^{65}Cu(30·83%), the isotopic contributions arise in the production of a given final nucleus through different reaction channels, for example ^{66}Ga is formed in ^{63}Cu(α, n) and ^{65}Cu$(\alpha, 3n)$ reactions and ^{65}Zn is formed in ^{63}Cu(α, pn) and ^{65}Cu$(\alpha, p3n)$ reactions respectively. However, more often than not, it turns out that at a given energy only one of the two reaction channels is predominant and the other is a small contribution. One of the two vanishes, if the energy happens to be less than the threshold energy for that reaction. On this basis the experimentally measured weighted average cross sections can be easily interpreted using the formula

$$\langle \sigma \rangle = \bar{A} \left(\frac{P_1 \sigma_1}{A_1} + \frac{P_2 \sigma_2}{A_2} \right) \tag{2}$$

Table 2. Cross sections of the α-induced reactions on $^{63,65}Cu$.

E_α(MeV)	(mb)	(mb)	(mb)	(mb)	(mb)	(mb)
Target nucleus reaction	^{65}Cu (α, n)	^{65}Cu $(\alpha, 2n)$	^{63}Cu (α, n)	$^{63}Cu + ^{65}Cu$ $(\alpha, n) + (\alpha, 3n)$	^{63}Cu $(\alpha, pn) + (\alpha, 2n)$	$^{63}Cu + ^{65}Cu$ $[(\alpha, pn) + (\alpha, 2n)] + [(\alpha, p3n) + (\alpha, 4n)]$
Product nucleus	^{68}Ga	^{67}Ga	^{66}Ga	^{66}Ga	$^{65}Zn + ^{65}Ga$	$^{65}Zn + ^{65}Ga$
Threshold Energy (MeV)	6·2	15·0	8·0	8·0, 26·9	13·4, 17·7	13·4, 17·7, 32·3, 36·6
11·6 ± 1·6			45·4 ± 3·8			
12·1 ± 1·1	315·0 ± 38·2					
14·3 ± 1·0	615·0 ± 74·5		197·0 ± 16·4			
16·4 ± 1·2	760·0 ± 92·4		417·0 ± 34·6			
17·3 ± 2·3	790·0 ± 95·8	72·0 ± 7·8	490·0 ± 40·7		64·0 ± 5·2	
20·2 ± 1·1	580·0 ± 70·3	475·0 ± 47·5	510·0 ± 42·3		260·0 ± 20·8	
21·5 ± 2·0		542·0 ± 54·2			530·0 ± 42·4	
22·6 ± 0·7	337·0 ± 40·9		327·0 ± 27·2		653·0 ± 52·3	
23·5 ± 0·9		860·0 ± 86·0			789·0 ± 63·2	
25·1 ± 1·7	206·0 ± 25·0	930·0 ± 93·0	181·0 ± 15·1		905·0 ± 72·4	
26·5 ± 0·9		1032·0 ± 10·3	126·0 ± 10·5		1013·0 ± 81·0	
28·4 ± 1·6	60·0 ± 7·8	943·0 ± 94·3			1040·0 ± 83·2	
29·0 ± 0·6					1085·0 ± 86·8	
31·6 ± 1·5	31·0 ± 4·1	762·0 ± 76·2		110·0 ± 9·2	960·0 ± 76·8	
34·5 ± 0·5	18·0 ± 2·4	560·0 ± 56·0		276·0 ± 22·9	780·0 ± 62·4	
37·1 ± 1·3	8·0 ± 1·1	380·0 ± 38·0		360·0 ± 30·0	554·0 ± 44·3	
39·6 ± 1·2	6·2 ± 0·8	254·0 ± 25·4		390·0 ± 32·4	437·0 ± 35·0	
42·1 ± 1·3	4·8 ± 0·6	183·0 ± 18·3		350·0 ± 29·0		
44·5 ± 1·1	3·2 ± 0·4	140·0 ± 14·0		292·0 ± 24·2		390·0 ± 31·2
46·7 ± 1·2	2·4 ± 0·3	108·0 ± 11·6		266·0 ± 22·0		452·0 ± 36·2
49·0 ± 1·0	2·0 ± 0·3	83·0 ± 8·9		216·0 ± 17·9		530·0 ± 42·4

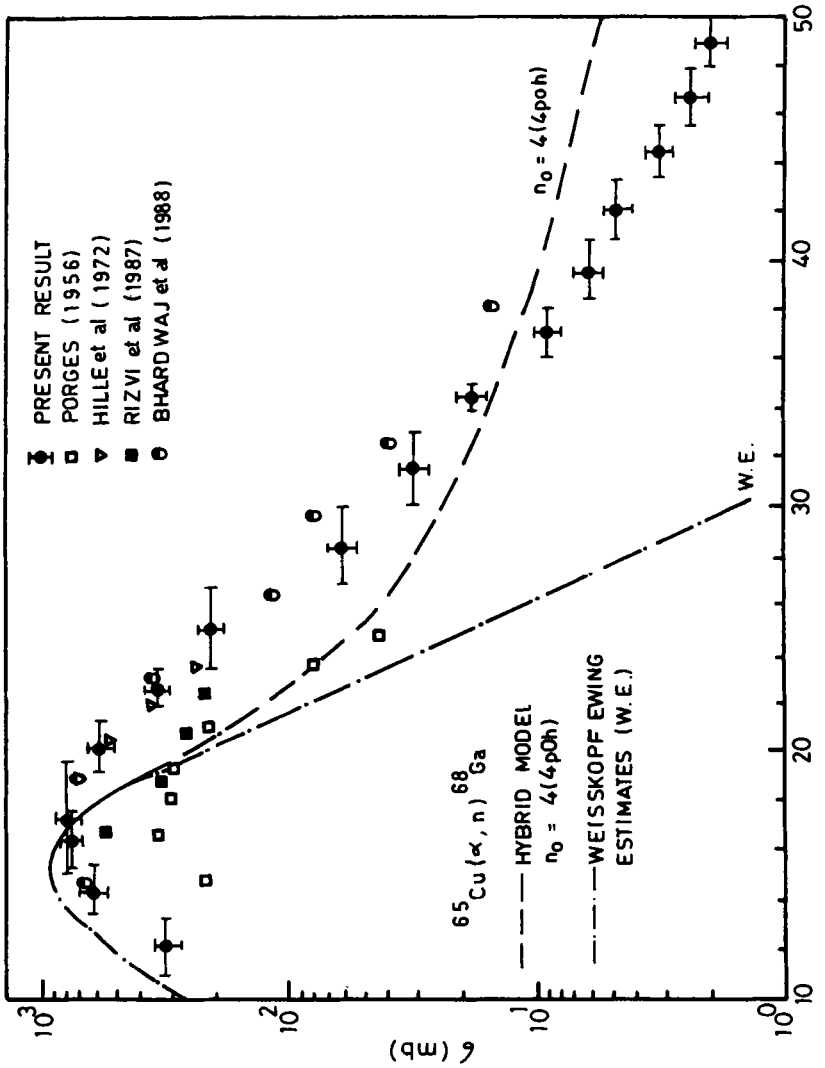

Figure 1. Excitation function of $^{65}Cu(\alpha, n)$ reaction.

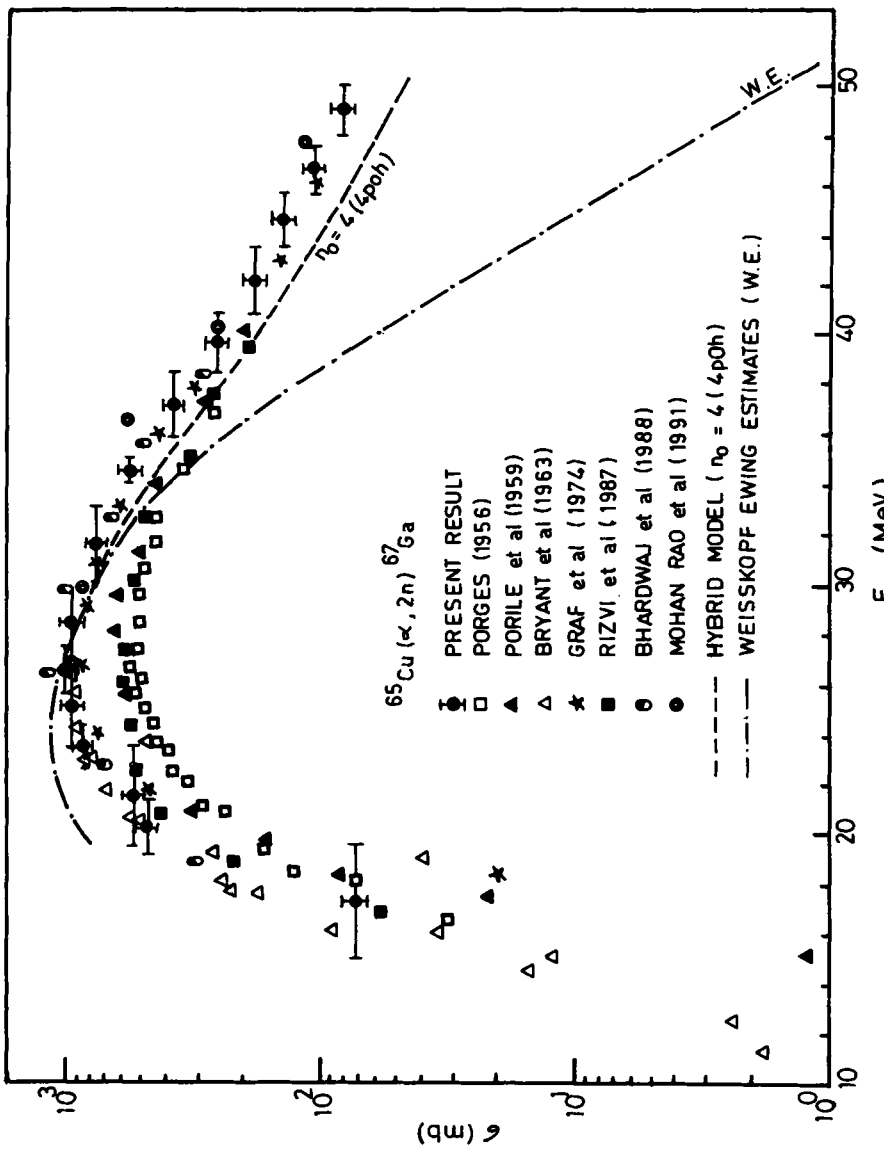

Figure 2. Excitation function of $^{65}Cu(\alpha, 2n)$ reaction.

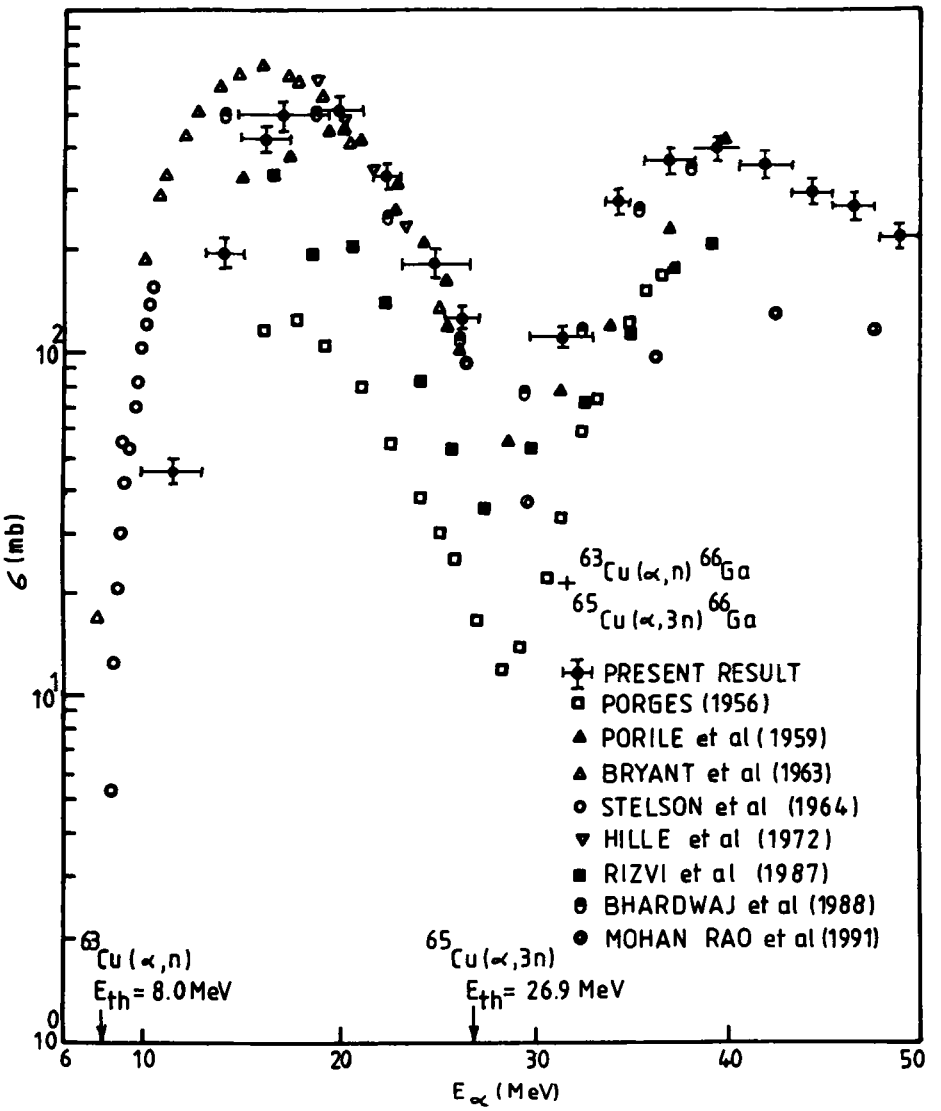

Figure 3. Excitation function of $^{63}Cu(\alpha, n) + {}^{65}Cu(\alpha, 3n)$ reactions.

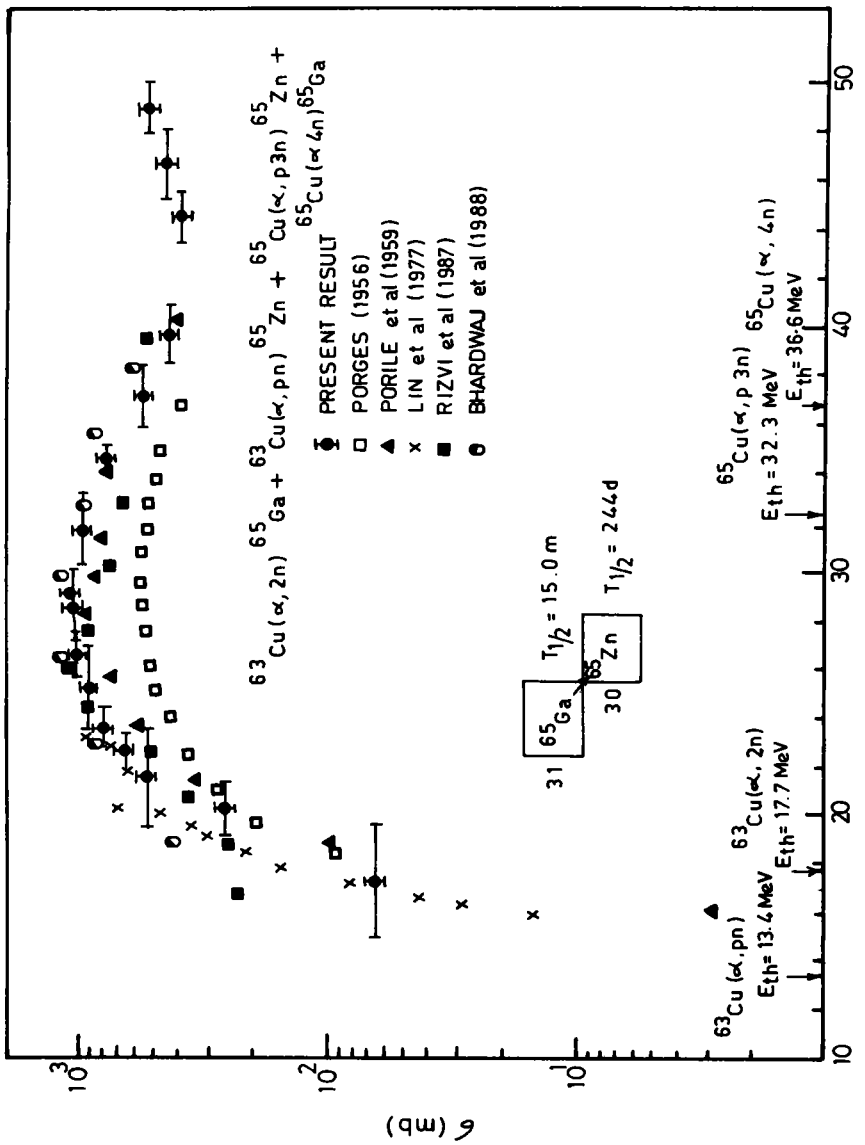

Figure 4. Excitation function of ^{63}Cu(α, 2n) + ^{63}Cu(α, pn) + ^{63}Cu(α, 4n) + ^{65}Cu(α, p3n) reactions.

where $\bar{A}$ is the average atomic weight of copper, P_1, A_1, and P_2, A_2 are the percentage abundances and mass numbers of the two isotopes of copper in respective order and σ_1, σ_2 are the individual cross-sections for $^{63}Cu(\alpha, n)$ and $^{65}Cu(\alpha, 3n)$ reactions respectively. The two contributions can be separated out accurately using either the known ratio of cross-sections from theory [26, 32, 33] or by subtracting out the contribution with enriched isotopes [34].

We have separated the individual contributions of the reactions employing the first method and using the theoretical ratio of cross-sections in formulae [32].

$$\sigma_1 = \sigma^{63}_{(\alpha,n)} = \frac{A_r \lambda}{\left[\frac{P_i^{63}}{A_i^{63}} + \frac{P_i^{65}(\sigma^{65}_{(\alpha,3n)}/\sigma^{63}_{(\alpha,n)})_{\text{theo.}}}{A_i^{65}}\right] \Phi\theta_r P_r w_i N_{av}(1 - e^{-\lambda t_i})e^{-\lambda t_w}(1 - e^{-\lambda t_c})} \tag{3a}$$

$$\sigma_2 = \sigma^{65}_{(\alpha,3n)} = \frac{A_r \lambda}{\left[\frac{P_i^{65}}{A_i^{65}} + \frac{P_i^{63}(\sigma^{63}_{(\alpha,n)}/\sigma^{65}_{(\alpha,3n)})_{\text{theo.}}}{A_i^{63}}\right] \Phi\theta_r P_r w_i N_{av}(1 - e^{-\lambda t_i})e^{-\lambda t_w}(1 - e^{-\lambda t_c})} \tag{3b}$$

where the cross-section ratio $(\sigma^{65}_{(\alpha,3n)}/\sigma^{63}_{(\alpha,n)})_{\text{theo.}}$ and its inverse are taken from the theoretical calculations based on pre-equilibrium model prediction, which predicts shape and absolute value of the excitation functions.

Below the threshold energy of $^{65}Cu(\alpha, 3n)$ reaction, the value of $\sigma^{65}_{(\alpha,3n)}$ will be zero and hence the second factor in the square bracket will be zero, therefore (3a) reduces to formula (1), (i.e. original formula).

Consequent on the use of natural copper as the target, two reactions are involved, in the production of the residual nucleus ^{66}Ga. Therefore, the experimental cross-section $\langle\sigma\rangle$ in this case gives the weighted average cross-section, for the two reactions $^{63}Cu(\alpha, n)$ and $^{65}Cu(\alpha, 3n)$. Below the threshold of $^{65}Cu(\alpha, 3n)$ reaction (i.e. 26·9 MeV), the measured excitation function is due to $^{63}Cu(\alpha, n)$ reaction only. The contribution of $^{63}Cu(\alpha, n)$ and $^{65}Cu(\alpha, 3n)$ reactions, beyond 26·9 MeV, was separated at each energy using formulae (3a) and (3b). This method for separating the two activities is justified, since the excitation function, for the reaction $^{63}Cu(\alpha, n)$ and for $^{65}Cu(\alpha, 3n)$ (figure 5), so resolved, are reproduced individually by theoretical calculation using the same set of parameters.

More often than not, nuclear reactions in which two genetically related product nuclei (e.g. isobars or isomers) are formed with comparable half-lives and one of them, the daughter nucleus being continuously fed by the parent for example, ^{65}Zn is produced by (i) $^{63}Cu(\alpha, pn)^{65}Zn$ and (ii) $^{63}Cu(\alpha, 2n)^{65}Ga \xrightarrow{\beta^+} {}^{65}Zn$. This is because ^{65}Ga decay with a relatively small half-life (15 min) into ^{65}Zn which in turn decays with a half-life of 244 days. In the present measurements a comparatively longer time was allowed between the end of the irradiation and the beginning of the counting and therefore the short-lived activity of ^{65}Ga was not observed separately.

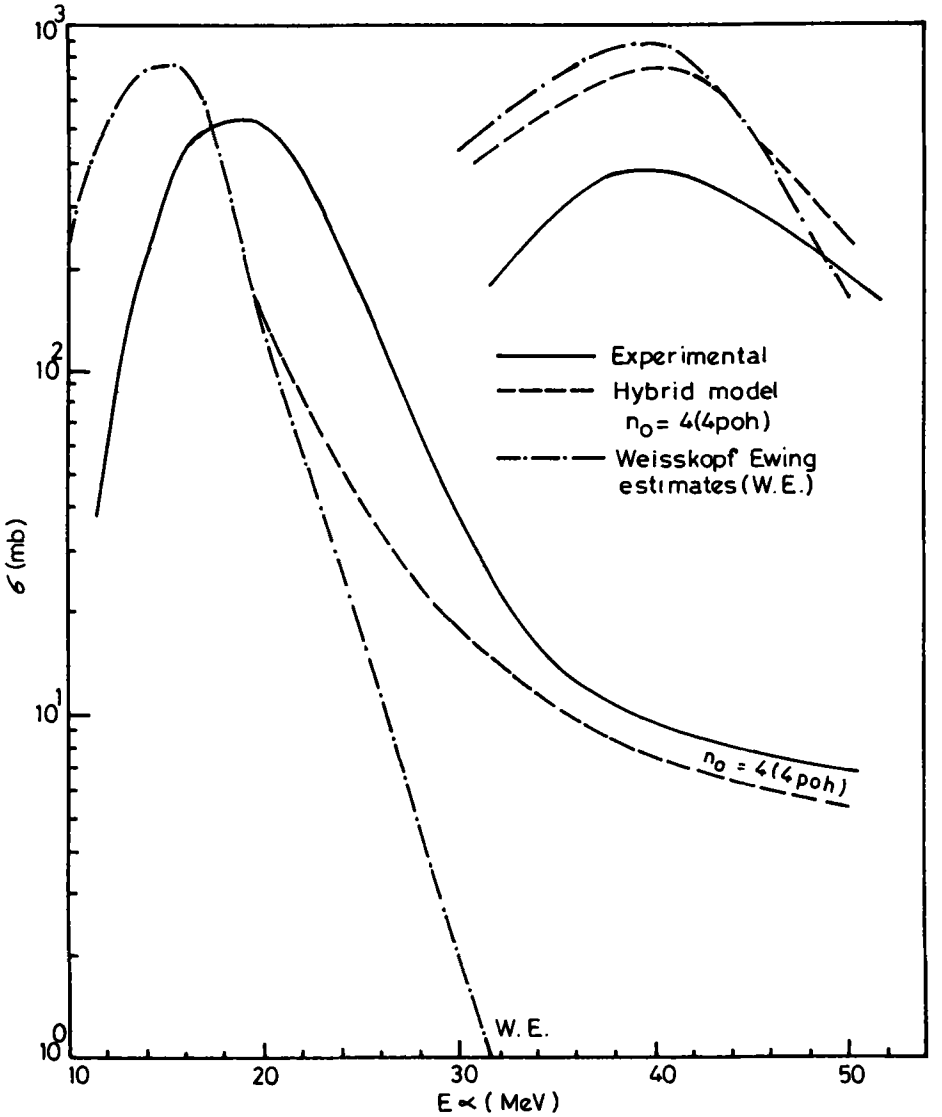

Figure 5. Experimental and theoretical excitation function of $^{63}Cu(\alpha, n)$ and $^{65}Cu(\alpha, 3n)$ reactions.

3.1 *Comparison of present and previous experimental results*

Figures 1–4 show the present experimental results together with the previous measurements. Most of the work on this element performed during 1956–1975, was carried out employing GM counter, scintillation detector, proportional counter as well as 4π flat energy response graphite sphere detector.

During the past twenty years, semiconductor radiation detector has become one of the principal tools in studies requiring high resolution measurements of gamma rays. There have been several Ge(Li) measurements of cross-sections but in limited energy regions [24–27]. It may be observed in figures 1–4 that while there is a fair

agreement between the present measurement and those of Graf *et al*, Bhardwaj *et al* and Mohan Rao *et al*, there are some disagreements between the present results and those of Rizvi *et al*.

It is appropriate to mention that the present experimental study adds nine new energy-point cross-sections in $^{65}Cu(\alpha, n)$, four new energy-point cross-sections in $^{63}Cu(\alpha, n) + {}^{65}Cu(\alpha, 3n)$ and three new energy-point cross-sections in $^{63}Cu[(\alpha, 2n) + (\alpha, pn)] + {}^{65}Cu[(\alpha, 4n) + (\alpha, p3n)]$ reactions in the high energy region.

3.2 *Comparison with pre-equilibrium model predictions*

The excitation functions have been calculated theoretically using the statistical model with and without the inclusion of preequilibrium emisson of particles using code ALICE/85/300 [35]. The forerunner for this model is the idea of Griffin [1] called as the statistical model of intermediate structure, to qualitatively explain the observed non-Maxwellian structure of continuous particle spectra. This model has been later quantified by deriving the unknown value of the matrix element for binary collision through various means. There are versions called exciton models in which the matrix element obtained semi-empirically [36] or through a picture of particle-hole interactions in a Fermi sea [5] or by simply treating it as a fit parameter [37]. An attempt to derive it from free nucleon–nucleon scattering cross-sections or from the imaginary part of the optical potential [4] resulted in what are popularly known as the hybrid model versions.

A short description of the option chosen is given below:

The nuclear masses were calculated from the Mayers and Swiatecki [38] mass formula considering the liquid drop without shell and pair corrections i.e. the level density pairing shift absorbed in binding energies. The inverse cross-sections were calculated by an optical model subroutine included into the code which uses the Becchetti and Greenless [39] optical model parameters. The equilibrium part was calculated using standard Weisskopf and Ewing [40] formalism. The mean-free-path was kept constant (i.e. $K = 1{\cdot}0$). The mean free path, which is a kind of free parameter, was introduced by Blann [3] to account for the transparency of nuclear matter in the lower density nuclear periphery. A level density parameter of $A/8\ MeV^{-1}$ was used.

A crucial parameter in the model is the initial exciton number n_0, defined as $n_0 = p_0 + h_0$ with $p_0 = p_\pi + p_\nu$, where p_0 and h_0 are initially excited particles above and holes below the Fermi sea, and p_π and p_ν are the number of protons and neutrons among the excited particles. It is customary to use the initial exciton number $n_0(p_0 h_0)$ as a fit parameter to match the theoretical predictions with the experimentally observed shape of spectra and excitation function. The initial exciton number governs the entire cascading process of binary collisions and thereby influences the shape of the hard component in the particle spectra. A good guess would be the number of nucleons in the projectile or an additional particle/hole or both. For the incident α-particle used in the present work a reasonable choice for the initial exciton number is $n_0 = 4$, 5 and 6 using different initial exciton configurations such as $(4p0h)$, $(5p0h)$ and $(5p1h)$ respectively [3, 41, 42]. We performed the calculations using the above exciton configurations and it was found that $n_0 = 4(4p0h)$ gives by far the best results than the other two configurations. The prediction of the $n_0 = 5(5p0h)$ and $n_0 = 6(5p1h)$ configurations were lower than those obtained with $n_0 = 4(4p0h)$. Figures 1, 2 and 5 show the comparison of experimental results with $n_0 = 4(4p0h)$ and Weisskopf–Ewing estimates.

Figures 1, 2 and 5 show the (α, xn) type of reactions on ^{63}Cu and ^{65}Cu; the experimental excitation functions of ^{65}Cu(α, n), ^{65}Cu$(\alpha, 2n)$, ^{63}Cu(α, n) and ^{65}Cu$(\alpha, 3n)$ reactions with the theoretical calculations based on the Weisskopf–Ewing estimates giving compound nucleus contributions as well as pre-equilibrium hybrid model prediction using $n_0 = 4(4p0h)$. The agreement between the experimental and the theoretical excitation functions can be judged from their peak positions and widths. It is observed that Weisskopf–Ewing estimates accounted fairly well for the lower energy compound nucleus dominated part of the excitation functions, but failed to account for the observed cross-sections at high energies where non-equilibrium effects predominate beyond a few tens of MeV of bombarding energy.

As can be seen from figures 1, 2 and 5 there is a slight shift in the energy of the compound nucleus peaks between the theoretical and experimental values. Generally such shifts are prescribed due to the complete neglect of angular momentum effects in the Weisskopf–Ewing theoretical calculations of the compound nucleus contribution. Compound systems attained with incident particles of different masses have appreciably different angular momenta when excited to the same excitation energy. This, in principle, can lead to differences in the excitation function. If, in the last stages of nucleon de-excitation, high angular momentum inhibits particle emission more than it does gamma ray emission, then the peak of the excitation function, corresponding to the particle emitting mode, will be shifted to the higher energy side. Such a shift could also be produced if the mean energy of the evaporated particles increases with increasing nucleon spin. The order of magnitude of this shift can be obtained from nuclear-rotational energy [43, 44]. More elaborate computations, using Hauser–Feshbach theory may bring about a better agreement. However, since the calculated inverse cross-sections depend critically on the optical model parameters and since there is no unique set of such parameters, a certain amount of uncertainty is inherent in the theoretical cross-sections.

In the case of (α, pxn) type of reactions, there are more complications due to isotopic contributions for a natural copper target. For example the long-lived ^{65}Zn$(T_{1/2} = 244\text{d})$ is formed not only in ^{63}Cu(α, pn) and ^{65}Cu$(\alpha, p3n)$ reactions but also by the β^+ decay of the 15 min ^{65}Ga. Which, in turn, is formed in ^{63}Cu$(\alpha, 2n)$ and ^{65}Cu$(\alpha, 4n)$ reactions. No attempt has been made in this case to separate out the isotopic contributions and to compare them with theory.

4. Fraction of pre-equilibrium particle emission

The present studies clearly show considerable pre-equilibrium contribution in α-induced reactions (figure 6). Pre-equilibrium fraction (f_{PE}) is a measure of the relative weights of the pre-equilibrium and equilibrium components needed to reproduce an experimental excitation function. It is defined as the integral pre-equilibrium neutron cross-section plus the pre-equilibrium proton cross-section divided by the total compound nucleus cross-section. This quantity is designated by f_{PE}. The calculated f_{PE} for ^{63,65}Cu are shown in figure 6 as a function of bombarding energy (E_α). It was found that f_{PE} increases very fast as the energy of the α-particle increases. Furthermore, the threshold for pre-equilibrium emission is higher for the lower mass number and f_{PE} is higher for the system of higher mass number at a given α-particle energy [45].

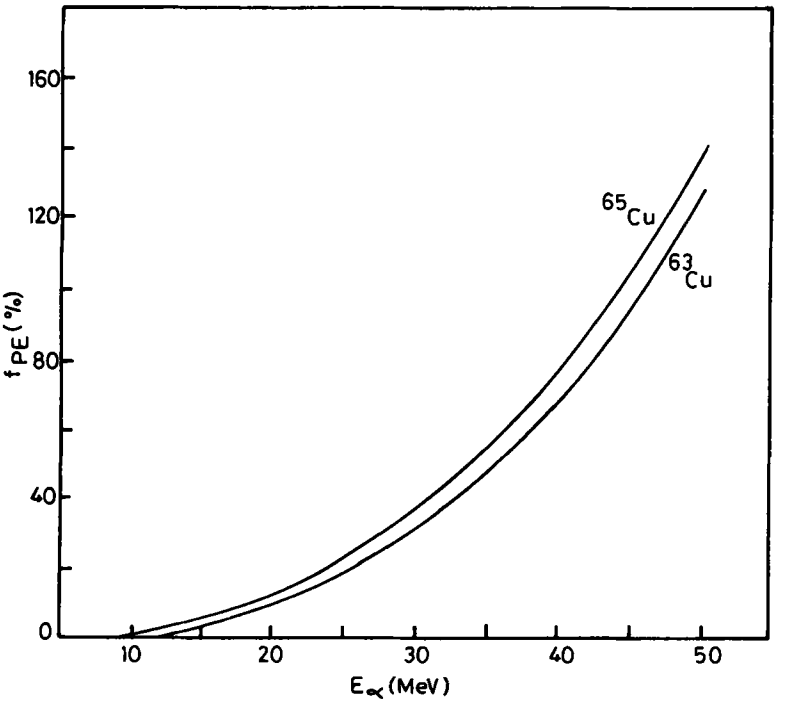

Figure 6. Pre-equilibrium fraction (f_{PE}) as a function of incident energy of alpha particle.

5. Conclusions

From an overall comparison of the experimental results and theoretical predictions based on compound nucleus Weisskopf–Ewing estimates as well as hybrid model, one can infer as in other works that the Weisskopf–Ewing estimate accounted well for the low energy compound nucleus dominated part of the excitation functions but failed to account for the observed cross-sections at higher energies, where non-equilibrium effects predominate beyond a few tens of MeV of bombarding energy. The basic tenet that only a small number of degrees of freedom is excited in pre-equilibrium reactions is amply borne out by the consistently good agreement observed between the experimental results and the pre-equilibrium predictions for an initial exciton number $n_0 = 4(4p0h)$. The physical interpretation of $n_0 = 4(4p0h)$ is that, only four excitons initially share the excitation energy and that these are particles above a completely filled Fermi-sea (i.e. pure particle state). The pre-equilibrium fraction (f_{PE}) for ^{63}Cu and ^{65}Cu has also been calculated. It is found that the pre-equilibrium reaction increases fast with the increase of incident α-particle energy. The threshold for pre-equilibrium emission is higher for lower mass number. It is also observed that the value of f_{PE} is higher for the system of higher mass number at a given α-particle energy.

Acknowledgements

We wish to express our sincere thanks to Prof. J Rama Rao and Dr S Mukherjee for stimulating discussions and help during the course of this work. We also thank the members of the cyclotron group for their cooperation. This work was supported by University Grants Commission (UGC), New Delhi.

References

[1] J J Griffin, *Phys. Rev. Lett.* **17**, 478 (1966)
[2] G D Harp, J M Miller and B J Berne, *Phys. Rev.* **165**, 1166 (1968)
[3] M Blann, *Phys. Rev. Lett.* **27**, 337; 700 E; 1550 E; (1971)
M Blann, *Ann. Rev. Nucl. Sci.* **25**, 123 (1975)
[4] M Blann and H K Vonach, *Phys. Rev.* **C28**, 1475 (1983)
[5] E Gadioli, E Gadioli-Erba and P G Sona, *Nucl. Phys.* **A217**, 589 (1973)
[6] J Ernst and J Rama Rao, *Z. Phys.* **A281**, 129 (1977)
[7] G Mantzouranis, D Agassi and H A Weidenmueller, *Z. Phys.* **A27**, 145 (1976)
[8] H Machner, *Phys. Lett.* **B86**, 129 (1979)
[9] J M Akkermans, H Gruppelaar and G Reffo, *Phys. Rev.* **C22**, 73 (1980)
[10] J Ernst, W Friedland and H Stoekhorst, *Z. Phys.* **A328**, 333 (1987); **A333**, 45 (1989)
[11] D Agassi, H A Weidenmueller and G Mantzouranis, *Phys. Rev.* **22**, 145 (1975)
[12] T Tamura, T Udagawa, D H Feng and K K Kan, *Phys. Lett.* **B68**, 109 (1977)
[13] L Avaldi, R Bonetti and L Colli Milazzo, *Phys. Lett.* **B94**, 463 (1980)
[14] H Feshbach, A Kerman and S Koonin, *Ann. Phys.* **125**, 429 (1980)
[15] G M Field, R Bonetti and P E Hodgson, *J. Phys.* **G12**, 93 (1986)
[16] P E Hodgson, Workshop on Applied Nuclear Theory and Nuclear Model Calculations for Nuclear Technology Applications, ICTP Report SMR/284-5 (1988)
[17] K G Porges, *Phys. Rev.* **101**, 225 (1956)
[18] N T Porile and D L Morrison, *Phys. Rev.* **116**, 1193 (1959)
[19] E A Bryant, D F Cochran and J D Knight, *Phys. Rev.* **130**, 1512 (1963)
[20] P H Stelson and F R McGrown, *Phys. Rev.* **B133**, 911 (1964)
[21] E Lebowitz and M W Greens, *Int. J. Appl. Radiat. Isot.* **21**, 625 (1970)
[22] M Hille, P Hille, M Uhl and W Weisz, *Nucl. Phys.* **A198**, 625 (1972)
[23] S Y Lin and I M Alexander, *Phys. Rev.* **C16**, 688 (1977)
[24] H P Graf and H Muenzel, *J. Inorg. Nucl. Chem.* **36**, 3647 (1974)
[25] I A Rizvi, M A Ansari, R P Gautam, R K Y Singh and A K Chaubey, *J. Phys. Soc. Jpn.* **56**, 3135 (1987)
[26] H D Bhardwaj, A K Gautam and R Prasad, *Pramana – J. Phys.* **31**, 109 (1988)
[27] A V Mohan Rao, S Mukherjee and J Rama Rao, *Pramana – J. Phys.* **36**, 115 (1991)
[28] C E Williamson, J P Boujot and J Picard, CENS Report, CEA-R 3042 (1966)
[29] C M Lederer and V S Shirley, *Table of isotopes* 7th edn. (John Wiley, New York, 1978)
[30] J Rama Rao, A V Mohan Rao, S Mukherjee, R Upadhyay, N L Singh, S Agarwal, L Chaturvedi and P P Singh, *J. Phys.* **G13**, 535 (1987)
[31] N L Singh, S Agarwal and J Rama Rao, *Can. J. Phys.* **71**, 115 (1993)
[32] N L Singh, S Agarwal, L Chaturvedi and J Rama Rao, *Nucl. Instrum. Methods* **B24/25**, 480 (1987)
[33] I A Rizvi, M K Bhardwaj, M A Ansari and A K Chaubey, *Can. J. Phys.* **67**, 870 (1989)
[34] P Misaelides and H Muenzel, J. Inorg. Nucl. Chem. **42**, 937 (1980)
[35] M Blann, Code ALICE/85/300 UCID-2069 (1984)
[36] C K Cline and M Blann, *Nucl. Phys.* **A172**, 225 (1971)
[37] H Stockhorst, W Friedland and J Ernst, *Proc. of the 3rd Int. Conf. on Nuclear reaction mechanism*, Verenna, June 14–19, Edited by E Gadioli (1982) pp. 119
[38] W D Mayers and W J Swiatecki, *Nucl. Phys.* **81**, 1 (1966)
[39] F D Becchetti and F W Greenless, *Phys. Rev.* **182**, 1190 (1969)

[40] V F Weisskopf and D H Ewing, *Phys. Rev.* **57**, 472 (1940)
[41] E Gadioli, E Gadioli-Erba, L Sajo-Bahus and G Tagliaferri, *Riv. Nuovo Cimenta.* **6**, 1 (1976)
[42] N L Singh, S Agarwal and J Rama Rao, *J. Phys. Soc. Jpn.* **59**, 3916 (1990)
[43] D Bodansky, *Ann. Rev. Nucl. Sci.* **12**, 79 (1962)
[44] M Blann and G Merkel, *Phys. Rev.* **B137**, 367 (1965)
[45] B P Singh, H D Bhardwaj, A K Gautam and R Prasad, *DAE Symp. Nucl. Phys.* **B35**, 232 (1992)